



Audio Engineering Society

Convention Paper 9770

Presented at the 142nd Convention
2017 May 20–23 Berlin, Germany

This Convention paper was selected based on a submitted abstract and 750-word precis that have been peer reviewed by at least two qualified anonymous reviewers. The complete manuscript was not peer reviewed. This convention paper has been reproduced from the author's advance manuscript without editing, corrections, or consideration by the Review Board. The AES takes no responsibility for the contents. This paper is available in the AES E-Library, <http://www.aes.org/e-lib>. All rights reserved. Reproduction of this paper, or any portion thereof, is not permitted without direct permission from the Journal of the Audio Engineering Society.

Perceptually Motivated Amplitude Panning (PMAP) for Accurate Phantom Image Localisation

Hyunkook Lee

Applied Psychoacoustics Lab, University of Huddersfield, Huddersfield, HD1 3DH, United Kingdom

Correspondence should be addressed to Hyunkook Lee (h.lee@hud.ac.uk)

ABSTRACT

This paper proposes and evaluates a new constant-power amplitude-panning law named ‘Perceptually Motivated Amplitude Panning (PMAP)’. The method is based on novel image shift functions that were derived from previous psychoacoustic experiments. The PMAP is also optimised for a loudspeaker setup with an arbitrary base angle using a novel phantom image localisation model. Listening tests conducted using various sound sources suggest that, for the 60° base angle, the PMAP provides a significantly better panning accuracy than the tangent law. For the 90° base angle, on the other hand, both panning methods perform equally good. The PMAP is considered to be useful for intelligent sound engineering applications, where an accurate matching between the target and perceived positions is important.

1 Introduction

Pairwise amplitude panning is currently the most popular technique to create and locate a phantom image at a specific position between loudspeakers. There are several laws available for panning in the conventional horizontal 2-channel stereo setup, for example tangent law [1], sine law [1] and cosine-sine law [2]. For surround (e.g., 5.1) and 3D (i.e., with height) formats, vector base amplitude panning (VBAP) is most widely used. The VBAP in 2-channel stereo is effectively the same as the tangent law.

The tangent and sine laws are primarily based on theoretical models that attempts to match the interaural time difference (ITD) produced by a phantom source to that by a real source at the target

position. The main difference between the two laws is that the tangent law takes into account the listener’s head rotation [1]. However, such ITD-based models are only valid up to about 700Hz since the ITD cue becomes ambiguous at higher frequencies [1]. Pulkki and Karjalainen [3] investigated the frequency dependency of the tangent panning with both subjective test and binaural modelling, and suggested that the localisation judgment using the tangent panning would rely on interaural level difference (ILD) cues at frequencies above about 2 kHz and ITD cues at frequencies below about 1 kHz. They found that the tangent law was inaccurate for frequencies between 1 kHz and 2 kHz. It has been shown that conventional panning methods tend to produce phantom images that are localised at a wider angle than the originally targeted angle, especially for broadband musical sources [2, 4]. Griesinger [2] asserts that such a discrepancy is due to the fact that

the position of a phantom image is determined by the frequency dependent averaging of various source locations, and that the human hearing system is most sensitive to frequencies between 700 Hz and 4 kHz. He further suggests that 1/3-octave frequency bands above 1 kHz are localised wider than targeted by the cosine-sine law due to the contribution of ILD and that this is the main reason for the broadband phantom source to be localised wider than targeted.

This paper proposes a novel constant-power amplitude panning law, which is named 'Perceptually Motivated Amplitude Panning (PMAP). The PMAP is developed based on phantom image shift factors that were derived from previous subjective listening tests using natural sources, and aims to provide a better localisation accuracy than the conventional theoretically-derived methods for 2-channel stereo. Furthermore, a novel binaural model is proposed to optimise the PMAP gain factors for an arbitrary loudspeaker base angle. The following sections explain the PMAP and the scaling method, followed by describing listening tests that were conducted to evaluate the method.

2 Proposed Method

This section describes the working principles for the proposed panning method, PMAP. A constant power panning law for the 60° loudspeaker base angle is first introduced, then the perceptual scaling approach to make the law applicable for an arbitrary base angle is presented.

2.1 PMAP for the 60° loudspeaker base angle

In the present author's previous study [5], interchannel level differences (ICLDs) required for locating a phantom image at 10°, 20° and 30° in the conventional 60° loudspeaker setup were measured subjectively using various types of musical sources. It was found that the ICLDs required for 10° and 20° image shifts increased linearly in general and that the ICLD difference between 20° and 30° shifts was almost double that between 10° and 20°. Furthermore, the panning uncertainty (i.e., the variance of ICLDs measured for a panning angle) was found to become greater at a wider angle. From

this, linear image shift factors were derived for two separate shift regions: 2.4°/dB for 0° to 20° and 1.2°/dB for 20° to 30° (e.g., 4.25dB for 10°, 8.5dB for 20° and 17dB for 30°).

From the above shift factors, the following relationship between target image angle α and the required ICLD and can be derived for the new panning method, PMAP.

$$ICLD(\alpha) = \begin{cases} 0.425\alpha, & |\alpha| \leq 20 \\ 0.85\alpha + 8.5, & -30 \leq \alpha < -20 \\ 0.85\alpha - 8.5, & 20 \leq \alpha < 30 \end{cases} \quad (1)$$

where ICLD is interchannel level difference of the right channel to the left channel. In constant power panning, the gain coefficients of the left and right channels g_1 and g_2 have the following relationship.

$$g_1^2 + g_2^2 = 1 \quad (2)$$

The ICLD of the right channel to the left can be expressed in terms of the gain coefficients as below.

$$ICLD = 20 \log_{10} \left(\frac{g_2}{g_1} \right) \quad (3)$$

From Equations 2 and 3, the gain coefficients for the PMAP can be described as

$$g_1 = \frac{1}{\sqrt{1 + 10^{\left(\frac{ICLD(\alpha)}{10}\right)}}}$$

$$g_2 = \sqrt{1 - g_1^2} \quad (4)$$

where ICLD is determined from Equation 1, depending on the desired panning angle α .

2.2 PMAP for an arbitrary base angle

Equation 1 is valid only for the $\pm 30^\circ$ 2-channel loudspeaker arrangement since it is based on subjective data obtained using the particular setup. More general PMAP functions for arbitrary loudspeaker base angles are provided below based

on two psychoacoustic considerations. Firstly, it is assumed that the linearity in image shift factor for the two separate panning regions, which was found for the 60° base angle, is still valid for different base angles. The two regions can then be generally described as 0 to 66.7% and 66.7% to 100%. Secondly, it is proposed that the ICLD required for a certain proportion of image shift for a specific base angle can be computed simply by applying a base-angle-dependent scale factor (sf) to Equation 1, which then can be rewritten as

$$ICLD(\alpha) = \begin{cases} sf(\theta) \left[0.425 \left(\frac{30\alpha}{\theta} \right) \right], & |\alpha| \leq \frac{2\theta}{3} \\ sf(\theta) \left[0.85 \left(\frac{30\alpha}{\theta} \right) + 8.5 \right], & -\theta \leq \alpha < -\frac{2\theta}{3} \\ sf(\theta) \left[0.85 \left(\frac{30\alpha}{\theta} \right) - 8.5 \right], & \frac{2\theta}{3} \leq \alpha < \theta \end{cases} \quad (5)$$

where θ is half the loudspeaker base angle and α is the target panning angle. sf is defined as the ratio of the average ILD above 1 kHz for the azimuthal position of one of the loudspeakers in reproduction (e.g., 45° for the 90° base angle) to that for 30°. This is based on the results of the ITD and ILD analyses of phantom and real sources for target image angles. The analyses used the ITD and ILD estimation model used by Pulkki and Karjalainen [3, 6]. HRIRs for different azimuth angles, taken from the MIT KEMAR database [7], were convolved with a 2048-sample-long white noise signal. The resulting signals then went through 42-channel Gammatone ‘equivalent rectangular band (ERB)’ filter bank. Half wave rectification and low-pass filtering at 1 kHz were applied to the filtered signals before ITD and ILD were estimated for each ERB channel. The ITDs were defined as the lag in millisecond where the maximum absolute value lies in the interaural cross-correlation function [8], whereas the ILDs were energy ratios between the left and right ear signals in dB. The average ITD was obtained for ERBs below the centre frequency of about 1 kHz, whereas the average ILD for those above about 1 kHz. Phantom sources for various target image positions were created at specific loudspeaker base angles according to Equation 5. It was found that the ILDs generally agreed well with those from real sources at the target positions (e.g., errors ranging

from 0dB to 0.6dB depending on the base angle and target angle), although the error ranges for ITDs were more considerable. It was hypothesised that the matching between real and phantom sources in the average ILD above 1 kHz would play a more important role for the phantom image localisation of broadband musical sources than those for the ITD below 1 kHz, since the human hearing is most sensitive at frequencies between 2 to 4 kHz and also most musical sources have spectral centroids above 1 kHz. The dominance of high-frequency ILD on phantom image localisation is discussed further in Section 3.6.

Figure 1 shows the scale factor as a function of loudspeaker base angle. For example, the sf for the 90° base angle is 1.3, since the ILD for the 45° azimuth is 1.3 times larger than that for the 30°. Hence, for the 90° loudspeaker setup, the ICLD required for a full image shift is 22dB, which is 1.3 times 17dB (the ICLD required for a full image shift for the 60° loudspeaker setup).

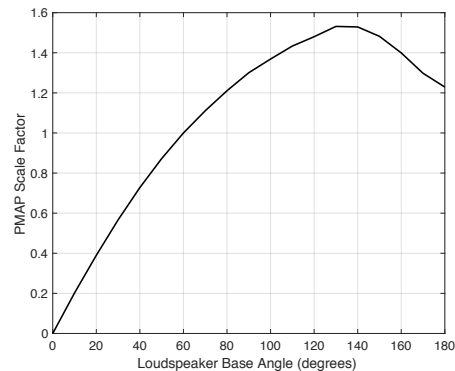


Figure 1. PMAP scale factor as a function of loudspeaker base angles.

3 Subjective Evaluation

Listening tests were conducted in order to evaluate the panning accuracy of the proposed method. A wide range of sound sources was chosen for the evaluation. Six panning angles were tested for the loudspeaker base angles of 60° and 90°. The original PMAP (i.e., Equation 1) was compared against the tangent law for the 60° base angle, whereas the scaled PMAP (i.e., Equation 5) was compared

against both the tangent law and the original PMAP for the 90° base angle.

3.1 Physical Setup

Listening tests were carried out in the ITU-R BS.1116-2-compliant critical listening room at the Applied Psychoacoustics Lab of the University of Huddersfield (T60 = 0.25s; NR 12). Two pairs of Genelec 8040A active loudspeakers were placed 2 m away from the listening position, one of which with the 60° base angle and the other with the 90°. The height of the acoustic centre (the middle point between the woofer and tweeter) was 1.3 m from the floor, which was also the height the listeners' ears were set to in the tests. Acoustically transparent curtains were placed in front of the loudspeakers to avoid any potential visual biases that might be caused during the listening tests.

In between the loudspeakers and the curtains, an arc-shaped thin wooden frame was placed and a strip of LEDs was attached on it. This was used for collecting the listeners' responses on the perceived image positions, which is a method originally proposed in [9]. The LED strip was controlled via an Arduino microcontroller and a graphical user interface (GUI) written using the Cycling'74 Max7 software. The total length of the strip was 5 m and there were 31 LEDs per metre. The distance between the listening position and the arc frame was 1.8 m. This gave the angular resolution of about 1° per LED from the listening position. The frame was placed just below the woofer height in order to avoid any potential high frequency diffraction. Frequency spectrum analysis showed that the acoustical effect of the frame was negligible.

3.2 Stimuli

A total of nine sound sources with different temporal and spectral characteristics were chosen for the tests. Six of them were the recordings of musical sources taken from the author's existing multitrack recording session: a female vocal, an acoustic guitar, a bass guitar, a kick drum, a snare drum and a trumpet. Each recording was made in a dry recording studio with a single microphone placed close to the instrument, thus having no audible reverberation.

The other three sources were a broadband pink noise burst (1 ms onset/offset; 200 ms duration; repeated every 1 second), the noise burst low-pass filtered at 1 kHz and that high-passed at 1 kHz (the 8th order linear phase Butterworth filter). All of the sources had the sampling frequency and bit depth of 44.1 kHz and 16bits, respectively.

For the 60° base angle (θ) test, 2-channel stimuli were created for the target panning angles of 5°, 10°, 15°, 20°, 25° and 30°, using both the original PMAP based on Equation 1 (referred to as PMAP60) and the tangent law. The target image angles for $\theta = 90^\circ$ were 7.5°, 15°, 22.5°, 30°, 37.5° and 45°. Stimuli for these were created using three methods: PMAP90 (the PMAP scaled based on Equation 5), the tangent law and PMAP60. The PMAP60 was included to examine whether the gain coefficients obtained for the 60° base angle would still be accurate for the 90° base angle.

3.3 Subject

13 subjects participated in the listening tests. They were staff members, post-graduate and undergraduate students of the music technology courses of the University of Huddersfield, whose ages ranged from 20 to 39. All of them reported normal hearing and had previous experiences in spatial audio listening tests.

3.4 Test Procedure

Each subject was to complete a total of five sets of listening test: PMAP60 for $\theta = 60^\circ$, tangent law for $\theta = 60^\circ$, PMAP90 for $\theta = 90^\circ$, tangent law for $\theta = 90^\circ$ and PMAP60 for $\theta = 90^\circ$. The order of the tests was randomised for each subject. Each test set comprised a total of 54 trials of a single stimulus (nine sources times six panning angles), whose order was randomised for each set and for each subject. Each test took about ten minutes to complete on average. However, no more than two tests were allowed to be done consecutively in order to avoid listener fatigue. There was at least five-minute break between two consecutive tests. At least one-hour gap was placed between two series of tests.

The subject was sit on a height-adjustable chair and their position was adjusted so that the ear height was 1.3 m and the distance between the ear and the loudspeaker was 2 m. In order to ensure that the listening position was correct, a phantom centre stimulus was played and it was checked if the subject localised the image at the 0° azimuth, which was visualised using an LED. A small head rest was put right at the back of the subject’s head to help him or her maintain the correct listening position. The subjects were instructed not to move their heads during the test and this was monitored by the author.

The subjects were given a USB-connected rotation knob (Griffin PowerMate), which they used to move the LED to the perceived position of the phantom image for each trial. By pressing the knob, the judged image position in degree was automatically saved in the Max7 GUI and the subject were moved onto the next trial.

3.5 Results

Shapiro-Wilk tests suggest that most conditions did not meet the assumption of normality for parametric statistical tests. Therefore, non-parametric tests were performed for the data analysis. Figure 2 plots the medians and associated interquartile ranges (IQRs) of differences of the perceived angle to the target angles (i.e., localisation errors) for each sound source and each target angle. The upper panel (a) is for for the 60° loudspeaker base angle, whereas the lower panel (b) for the 90° base angle. Wilcoxon’s one-sample signed rank tests were performed to examine whether each median perceived angle was significantly different from the target angle; if not significant, it can be suggested that the phantom image would be localised accurately. In order to examine the main effects of panning method, sound source and perceived angle, Friedman’s analysis of variance (ANOVA) tests and Wilcoxon’s related-sample signed-rank tests were performed. The cut-off p value used for significant testing was 0.05.

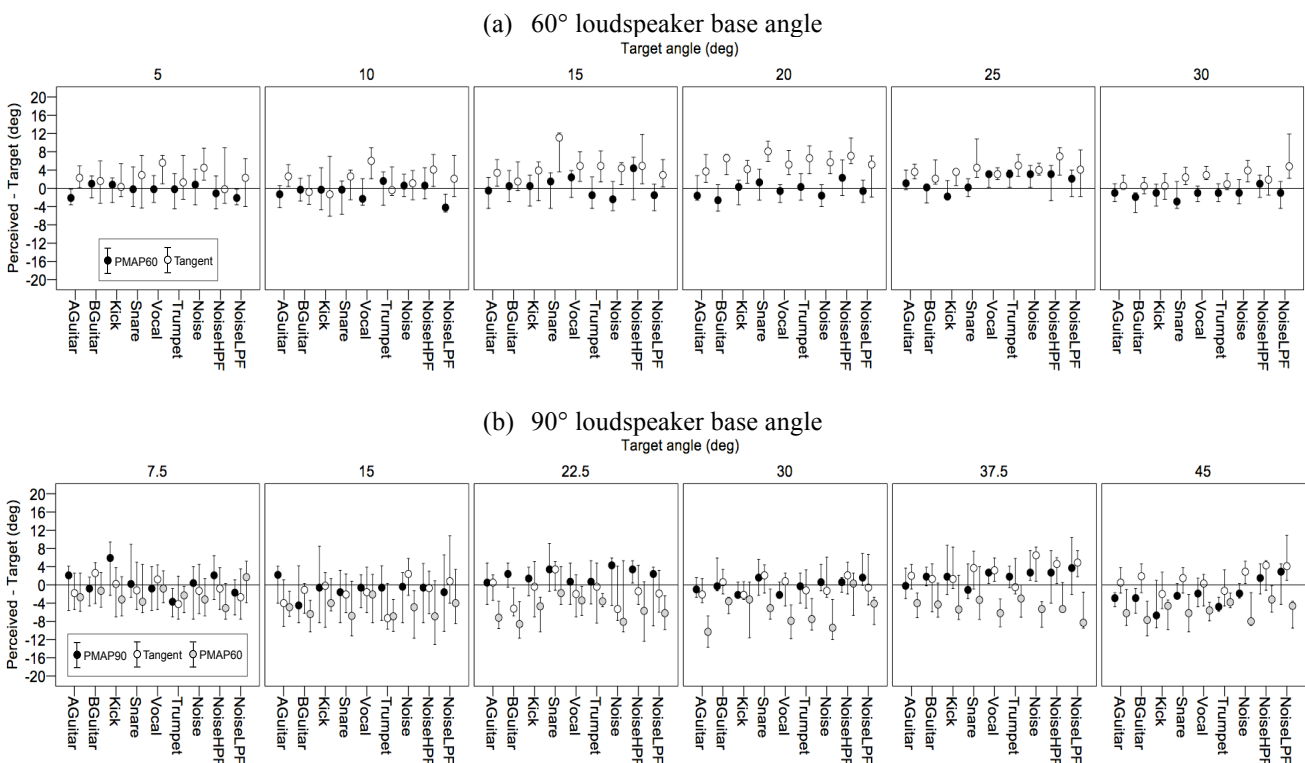


Figure 2. Medians and associated interquartile ranges (IQRs) of the differences of perceived angles to target angles for individual sources, separately plotted for each target angle: (a) 60° loudspeaker base angle; (b) 90° loudspeaker base angle.

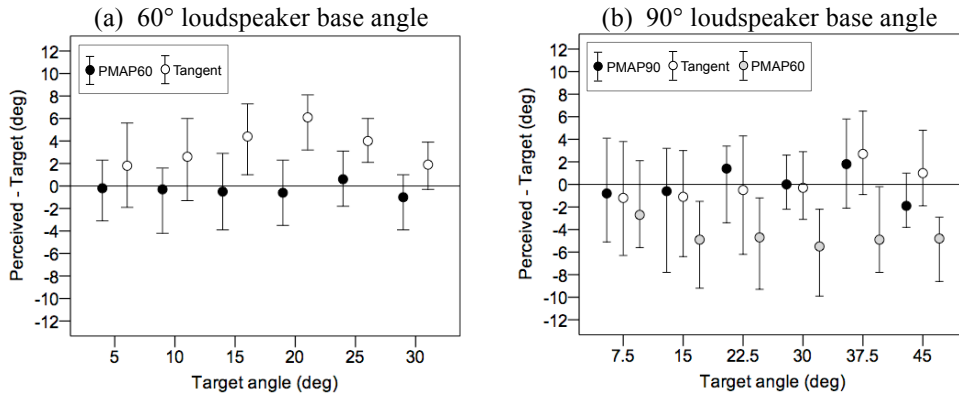


Figure 3. Medians and associated interquartile ranges (IQRs) of the differences of perceived angles to target angles for all sources: (a) 60° loudspeaker base angle; (b) 90° loudspeaker base angle.

3.5.1 60° loudspeaker base angle

The main effect of the panning method was found to be significant ($p < 0.01$) for all target angles. In Figure 2(a), it generally appears that the PMAP60-panned images were localised accurately for most of the sources for all target angles. On the other hand, the tangent-panned images tend to demonstrate upper biases in localisation, which agrees with previous findings on the accuracy of the tangent law [2,4].

The one-sample Wilcoxon test showed that, for the 5° angle, the PMAP60 produced an accurate localisation for all sources (i.e., non-significant difference between the target and perceived angles, $p > 0.05$) except the acoustic guitar and the low-passed noise, which had slight but significant lower biases ($p < 0.01$). The tangent law for the 5° target angle was accurate for all sources apart from the vocal and the broadband noise ($p < 0.01$). For the 10° target, only the low-passed noise had a significant lower bias for the PMAP60 ($p < 0.01$), whereas the vocal and the high-passed noise had significant upper biases for the tangent law ($p < 0.05$). The 15° and 20° target angles had more obvious differences between the two panning methods than the narrower angles. For 15°, the PMAP60 had no significant localisation error for all

sources ($p < 0.05$), whereas the tangent law had significant errors for all sources except the low-passed noise. For 20°, the bass guitar was the only source that had a significant inaccuracy for the PMAP60, whereas all sources were inaccurately localised for the tangent law ($p < 0.05$). For 25°, the PMAP60 was accurate except for the vocal, trumpet and broadband noise sources, whereas the tangent law was not for any source. For 30°, the PMAP60 had a significant difference for the base guitar and snare sources, whereas the tangent law for the vocal, the snare and the broadband and low-passed noise sources.

Figure 3(a) shows the medians and IQRs of localisation errors plotted for the data from all sources. It can be seen that the error is noticeably smaller with the PMAP60 for all target angles. The errors for the PMAP60 were within $\pm 1^\circ$ of median angles, which was not significant for all target angles except 25°. On the other hand, the tangent law had significant errors for all angles, with the largest being 6° for the 20° target.

3.5.2 90° loudspeaker base angle

It was found that all target angles except the 7.5° had a significant effect of the panning method. Bonferroni-corrected pairwise comparisons revealed that for the target angles from 7.5° to 45°, the

PMAP60 was significantly different from the PMAP90 and the tangent law ($p < 0.01$). The differences between the PMAP90 and the tangent law were non-significant for all target angles except 45° .

The one-sample Wilcoxon tests suggest that for the 7.5° the median differences between the perceived and target angles (i.e., localisation error) were not significant for all sources for both the PMAP90 and tangent law. On the other hand, the PMAP60 had significant localisation errors (lower biases) for the trumpet and high-passed noise sources ($p < 0.05$). For the 15° target, the PMAP90 did not produce significant localisation errors for any source, whereas the tangent law produced significant localisation errors for the acoustic guitar and the trumpet ($p < 0.05$), and the PMAP60 for the trumpet ($p < 0.01$), broadband noise ($p < 0.05$) and high-passed noise ($p < 0.05$). The sources that had significant localisation errors for the 22.5° target for the PMAP90 were the snare ($p < 0.05$) and the high-passed noise ($p < 0.01$), whereas that for the tangent law was the base guitar ($p < 0.05$). The PMAP60 produced significant lower biases in localisation for all sources apart from the snare and the broadband noise. For the 30° target, the tangent law did not produce significant localisation errors for any source. For the PMAP90 only the low-passed noise had a significant localisation error ($p < 0.05$), whereas the PMAP60 had significant errors except for the kick and high-pass noise sources. For the 37.5° target, the PMAP90 produced a significant median difference only for the broadband noise ($p < 0.05$), whereas the tangent for the broadband, low-passed and high-passed noise sources and the PMAP60 for the acoustic guitar, bass guitar, vocal, broadband noise and low-passed noise sources. For the 45° target, the acoustic guitar, bass guitar, kick and trumpet sources had significant localisation errors with the PMAP90, whereas the low-passed and high-passed noises with the tangent law. For the PMAP60, all sources except the high-passed noise had significant localisation errors.

Figure 3(b) shows the medians and IQR plotted for the data from all sources for each target angle. Overall, it appears that the PMAP90 and the tangent

law had similar degrees of localisation errors for all target angles overall, whereas the PMAP60 had noticeably greater errors towards the lower angles than the other two methods. The range of median errors across all target angles were -1.9° to 1.4° for the PMAP90, -1.2° to 2.7° for the tangent law and -5.5° to -2.7° for the PMAP60. These errors were statistically significant ($p < 0.01$) for all angles for the PMAP60. For both the PMAP60 and the tangent law, the errors were significant ($p < 0.05$) for all target angles other than 7.5° and 30° .

3.6 Discussion

From the results, it can be suggested that the PMAP60 produces more accurately panned images than the tangent for the 60° loudspeaker base angle. The tangent law suffered from significant upper biases, which agrees with the literature [2,4], and this tendency was found to be particularly stronger at the target angles of 15° and 20° . The tangent law relies on the matching between real and phantom sources in ITD at frequencies below about 700 Hz. On the other hand, the PMAP60 is derived from previous subjective listening tests that measured ICLDs required for panning phantom images of musical sources at specific angles in the 60° loudspeaker setup.

In order to explain the subjective results based on objective parameters, average ITDs below 1 kHz and average ILDs above 1 kHz were computed for phantom images at target angles up to 25° using the ERB-based binaural model described in Section 2.2. For the 60° base angle and 30° target angle condition, there is no difference between the tangent-panned source and the real source at 30° in ITD and ILD as the tangent law applies an infinite ICLD for this target angle. It is worth noting that the PMAP also produces almost identical average ILD for this target angle (0.1 dB error) – this is achieved by the PMAP applying 17 dB of ICLD. For the 10° and 20° target angles, on the other hand, the tangent produced substantially larger ILD errors than the PMAP, e.g., the tangent law produced 1.2 dB and 1.43 dB more ILDs than the real sources at 10° and 20° , respectively, whereas the PMAP had 0.41 dB and 0.3 dB differences to the same real sources. On the other hand, the ITD errors for the target angles

were larger with the PMAP in general; the PMAP had around 0.1 ms of ITD error for the 10°, 20° and 30° target angles, whereas the tangent law had almost no error for the same angles. Considering the subjective results showing that the PMAP was more accurate than the tangent law for the 60° base angle, the ITD and ILD analysis results seem to confirm the original hypothesis that high-frequency ILD matching between the real and phantom sources play a more important role on phantom image localisation than the low-frequency ITD matching.

The subjective results from the 90° base angle test indicate that the proposed scaling method for the PMAP (Section 2.2) performed well. Both the PMAP90 and tangent law produced similar degrees of localisation errors in general (around ± 2 dB) as well as the same statistical significances for all target angles. The analyses of ITD and ILD suggests that the differences between the two methods in average ILD error are generally minimal for the 15° (0.5 dB), 30° (0.1 dB) and 45° (0 dB) target angles. Differences between the methods in ITD error were almost none for the 15° and 30°, but that for the 45° (0.1 ms) might be considerable. In fact, the subjective results also show that the PMAP90-panned images tended to be perceived at slightly narrower angles than the tangent-panned images.

Additionally, the result showing that the PMAP60 did not perform well for the 90° base angle suggests that the ICLD required for a certain portion of phantom image shift depends on the loudspeaker base angle. This disagrees with the literature [10,11] suggesting that the ICLD-shift factor relationship is constant regardless of the base angle.

4 Conclusion

In this paper, a novel constant-power amplitude panning method named ‘Perceptually Motivated Amplitude Panning (PMAP)’ was proposed. The PMAP is based on a relationship between ICLD and phantom image shift factors for musical sources, established from previous listening tests using the 60° loudspeaker base angle [5]. A novel scaling approach to make the PMAP generally applicable for an arbitrary base angle was devised based on an

ERB-based ITD and ILD analysis. Subjective listening tests were conducted to evaluate the panning performances of the PMAP and the tangent law for the 60° and 90° base angles using nine different sound sources. For the 90° base angle, the scale factor of 1.3 was applied to the original PMAP. The results showed that for 60° the PMAP was more accurate than the tangent law overall. On the other hand, both methods demonstrated similar panning accuracies for 90° in general. Additionally, the original PMAP was found to produce inaccurate results for the 90° base angle, which suggests that ICLD-image shift relationship is dependent on the base angle. Finally, ERB-based binaural analyses were conducted to measure ITDs and ILDs resulting from both real and phantom conditions. It was found that the PMAP-panned sources had smaller differences to the corresponding real sources in average ILDs above 1 kHz compared to the tangent-panned ones, whereas the formers had larger differences in ITDs below 1 kHz than the latter. This seems to suggest that the high-frequency ILD influences subjective localisation of phantom image more than the low-frequency ITD.

5 Acknowledgment

The author is grateful to all the staff members and students of the music technology courses at the University of Huddersfield who participated in the listening tests. He also thanks Chris Gribben, who wrote the GUI used for the listening tests.

References

- [1] D. M. Leakey, “Some measurements on the effect of interchannel intensity and time difference in two channel sound systems,” *J. Acoust. Soc. Am.*, vol. 31, pp. 977–986 (1959 July).
- [2] D. Griesinger, “Stereo and Surround Panning in Practice,” *presented at the 112th Convention of the Audio Engineering Society* (2002 May), convention paper 5564.
- [3] V. Pulkki, and M. Karjalainen, “Localization of Amplitude-Panned Virtual Sources, II:

- Two- and Three- Dimensional Panning,” *J. Audio Eng. Soc.*, vol. 49, pp. 753–767 (2001 Sep.).
- [4] T. Choi, Y. Park, D. Youn and S. Lee, “virtual sound rendering in a stereophonic loudspeaker setup,” *IEEE Trans. Audio, Speech, Language Process.*, vol. 19, pp. 1962–1974 (2011 Sep.).
- [5] H. Lee and F. Rumsey, “Level and time panning of phantom images for musical sources,” *J. Audio Eng. Soc.*, vol.61 (12), pp. 753–767 (2013 Dec.).
- [6] V. Pulkki and M. Karjalainen, *Communication Acoustics: An Introduction to Speech, Audio and Psychoacoustics* (Wiley, 2015).
- [7] B. Gardner and K. Martin, URL: <http://sound.media.mit.edu/resources/KEMAR.html>. 2000.
- [8] D. J. Kistler and F. L. Wightman, “A model of head-related transfer functions based on principal components analysis and Minimum-phase reconstruction,” *J. Acoust. Soc. Am.*, vol. 91, pp. 1637–1647 (1992).
- [9] H. Lee, D. Johnson and M. Mironovs, “A new response method for auditory localisation and spread tests,” *presented at the 140th Convention of the Audio Engineering Society* (2016 June), engineering brief 240.
- [10] M. Williams, “Unified theory of microphone systems for stereophonic sound recording,” presented at the *82nd Convention of the Audio Engineering Society* (1987), convention paper 2466.
- [11] G. Theile, “Multichannel natural recording based on psychoacoustic principles,” In *Proceedings of the Audio Engineering Society 19th International Conference*, pp. 201–229 (2001).